Composites: Part A 146 (2021) 106415

Contents lists available at ScienceDirect

Composites Part A

journal homepage: www.elsevier.com/locate/compositesa

Water resistant fibre/matrix interface in a degradable composite: Synergistic effects of heat treatment and polydopamine coating

Reda M. Felfel [a,c,*,1], Andrew J. Parsons [b,1], Menghao Chen [a], Bryan W. Stuart [a], Matthew D. Wadge [a], David M. Grant [a]

[a] Advanced Materials Research Group, Faculty of Engineering, University of Nottingham, Nottingham, UK
[b] Composites Research Group, Faculty of Engineering, University of Nottingham, Nottingham, UK
[c] Physics Department, Faculty of Science, Mansoura University, Mansoura 35516, Egypt

ARTICLE INFO

Keywords:
Glass fibres
Surface treatments
Thermoplastic resin
Fibre/matrix bond

ABSTRACT

Retaining a robust fibre-matrix interface in an aqueous environment has been an enduring challenge for fibre-reinforced biocomposites. This study addresses the issue by applying a polydopamine coating as a coupling agent to annealed and non-annealed phosphate-based glass fibres. The presence of the polydopamine coating was confirmed using X-ray photoelectron spectroscopy and Raman techniques. The thickness of the coating increased with treatment time, forming a bimodal structure, and showed good correlation with the percentage of surface nitrogen observed via XPS. A 6 h coating period was selected to balance fibre strength improvements against degradation caused by the aqueous coating solution. In-situ polymerised polycaprolactone composites were produced using the fibres, resulting in improved retention of strength and modulus when the fibres were both annealed and coated. This is the first example of long-term retention of wet strength properties for phosphate-based glass fibre composites, falling within the target range for bone healing (6–12 weeks).

1. Introduction

The development of effective absorbable composites is an important step in developing new materials for both high value, low production volumes (e.g. medical device products) and for commodity, high production volumes (e.g. automotive components and packaging). In both cases the initial mechanical properties must achieve target in-situ requirements, followed subsequently by a controlled loss of properties. In the case of medical devices this is to facilitate a gradual transfer of load to healing bones, whilst for commodity products this is a key part of sustainability through recycling or composting.

Phosphate-based glasses have been developed as reinforcing fibres for absorbable composites [1–10]. They can provide properties on a par with traditional glass fibre composites, but are also soluble in water at controllable rates. While there have been studies that show great promise for the dry properties of phosphate glass composites, maintaining properties during degradation is challenging.

The key to this issue lies in the fibre/matrix interface. Composite properties rely on a strong bond between fibre and matrix that allows for stress transfer; if the bond is poor then the properties are commensurately poor. Phosphate glass fibres (PGF) degrade via surface erosion [11–13]. This means that, since the matrix will allow the passage of water (~1% absorption in PLA), the first part of the composite to degrade is the fibre/matrix interface. This can be seen in a number of studies, where the composite properties fall by 30–50% within the first few days in an aqueous environment even though the fibres do not appear significantly degraded [14–16].

This can be addressed to some degree by improved manufacturing conditions. Studies using in-situ polymerisation methods for polycaprolactone (PCL)/PGF composites have observed much improved initial properties over a conventional laminate stacking/hot pressing process (~10–40% improvements in strength and modulus) [17]. This is because in-situ polymerisation achieves a much better wet-out of the fibres and consequently a better fibre/matrix interface. Although there is clear improvement, the effect is not prolonged beyond two weeks. In medical device applications – the principle target sector for phosphate glass composites – properties need to be maintained for 6–12 weeks to allow healing time [18]. For commodity products, in-situ

* Corresponding author at: Wolfson Building, Faculty of Engineering, University of Nottingham, University Park, Nottingham, NG7 2RD, UK.
E-mail address: reda.felfel@nottingham.ac.uk (R.M. Felfel).
[1] These authors contributed equally.

https://doi.org/10.1016/j.compositesa.2021.106415
Received 8 November 2020; Received in revised form 23 March 2021; Accepted 3 April 2021
Available online 15 April 2021

polymerisation methods are impractical at present due to scale and cost but there is considerable interest in their development, particularly for lactams [19,20].

The most common route to improve the fibre matrix interface is by the use of chemical treatments and the inclusion of coupling agents [21,22]. These are usually surfactant-type compounds that will bond to the fibre with one functional group and to the matrix with another and they are used in almost all composites, absorbable or not. Silanes are the most well-known coupling agents in glass fibre composites and they have been investigated in phosphate glass composites with mixed results [23–28]. This is not wholly unexpected, since phosphates and silicates do not form good shared structures. A wide variety of other materials have been assessed as chemical treatments for phosphate glass fibres, though to date none have been effective in extending property lifetimes by any significant degree [3,25,26,29–32].

Finally, the fibre itself can be modified to try and improve the composite properties. Fibre compositions can be produced that are more durable and the fibres can be annealed to remove residual stresses [33]. Fibre surfaces can also be modified to increase surface roughness to promote mechanical interlocking [31,34]. However, more durable phosphate compositions tend to be difficult to convert to fibre and both annealing (heat treatment) and surface roughening can incur a penalty in fibre strength by exacerbating flaws [35]. In either case the benefits to hydrolysis resistance have been limited.

The present study reports on the use of a new fibre chemical treatment with the potential to substantially improve the interface between fibre and matrix in absorbable phosphate glass composites. The treatment involves the application of polydopamine to the fibre surface. Dopamine is from the catecholamine group of compounds and occurs naturally in plants and animals as a neurotransmitter. However, when dopamine is placed in an alkaline environment it can form polydopamine (PD) and is effective in coating a wide range of materials [36], although the structure of the polymer has not yet been fully elucidated. Polydopamine coatings have been shown to be effective biocompatible adhesives and are particularly good in protein bonding. Further, they have been used to enhance the effects of interfacial adhesion in a range of different fibre-reinforced composites, achieving significant improvements in dry strength and modulus for carbon, glass and polymer fibres [37–42]. However, it has not yet been utilised in an absorbable composite system. If the PD provides good interfacial adhesion that persists in an aqueous environment, it could be an effective coupling agent for absorbable composites.

As well as assessing the effectiveness of polydopamine as a coupling agent by itself, this study also considers combination solutions to the fibre/matrix interface issue. The polydopamine treatment is performed in conjunction with fibre annealing and composites are produced via an in-situ polymerisation process.

2. Methodology

2.1. Materials

Dopamine hydrochloride, tris buffer, ε-caprolactone monomer, benzyl alcohol initiator, $Sn(Oct)_2$ catalyst and all the required glass making salts were purchased from Sigma Aldrich (UK).

2.2. Fibre production and coating

Glass of composition 45 mol% P_2O_5, 24 mol% MgO, 16 mol% CaO, 10 mol% Na_2O and 5 mol% Fe_2O_3 was produced by melting at 1150 °C for 1.5 h in a platinum alloy crucible and then quenching by pouring into a steel mould. Afterwards, the glass was re-melted and drawn into fibres (25 ± 5 μm diameter) at *ca.* 1200 °C and 300 m per minute using an in-house facility [17].

A portion of the fibres was kept in a desiccator and the rest were annealed at 479 °C (T_g, −5 °C) for 90 min. Amounts of the annealed and non-annealed fibres were coated with polydopamine following the process introduced by Lee et al [36]. The fibres were aligned and fastened onto a plastic mesh using soft rubber bands to avoid fibre damage and breaking during the coating process (see Fig. 1). The mesh and fibres were then immersed in dopamine hydrochloride aqueous solution (2 mg/mL in 10 mM tris, pH ~ 8.5) for different periods of time; 0.5, 3, 6 and 24 h. At each time point, the fibres were removed from the dopamine solution and washed carefully with distilled water to remove any unreacted dopamine on the fibre surface. The fibres were then dried overnight at 50 °C. Finally, the coated and non-coated fibres were kept in a desiccator prior to fibre testing and composite manufacturing.

2.3. Composites manufacturing via in-situ polymerisation

The in-situ polymerisation method for PCL based fibre reinforced composites is an established method [28,43–45] but has only recently been refined for PGF [17]. Briefly, PGFs were cut to fit a PTFE mould cavity (130 mm × 165 mm × 2 mm). They were aligned unidirectionally (UD) and the amount of fibres was adjusted to obtain a fibre volume fraction (V_f) of 35%. A solution of ε-caprolactone was prepared with a concentration of 8.68 mmol/l $Sn(Oct)_2$ catalyst and 11.59 mmol/l benzyl alcohol initiator under dry nitrogen gas, with a target molecular weight (M_w) of 90 kDa. The solution was injected into the mould cavity at room temperature and the mould was moved to a preheated oven at 130 °C for 24 h.

The resulting PCL-PGF composite plate was cut using a band saw into specimens that were 40 mm long, 15 mm wide and 2 mm thick. Four different composite types were manufactured, as listed in Table 1. Volume fraction was confirmed via burn off analysis using BS EN ISO 2782-10 (n = 5).

2.4. X-ray photoelectron spectroscopy (XPS)

XPS was conducted using a VG Scientific EscaLab Mark II with an Al Kα non-monochromatic X-Ray Source. Scans were collected at 20 mA and 12 kV emissions, with the following parameters: step size 0.2, replicate scans = 5, and dwell times of 0.4 s per step. Charge correction calibration was observed at 284.8 eV for the C 1s peak. Analysis and peak fitting were conducted using CasaXPS software, with the application of a Shirley background subtraction. The Full Width was constrained at Half Maximum for all convolutions of the same element.

2.5. Micro-Raman spectroscopy

Raman spectroscopy was performed using a HORIBA Jobin Yvon LabRAM HR spectrometer. Spectra were acquired using a 532 nm laser at 25 mW power, a 50× objective and a 300 μm confocal pinhole. To simultaneously scan a range of Raman shifts, a 600 lines/mm rotatable diffraction grating along a path length of 800 mm was employed. Spectra were detected using a SYNAPSE CCD detector (1024 pixels) thermoelectrically cooled to −60 °C. Prior to spectral collection, the instrument was calibrated using the Rayleigh line at 0 cm^{-1} and a standard Si (100) reference band at 520.7 cm^{-1}. Spectra were recorded for 10 s with 10 accumulations per sample.

2.6. Atomic force microscopy (AFM)

AFM micrographs and roughness measurements were acquired in tapping mode via a Bruker Dimension Icon Atomic Force Microscope equipped with antimony (n) doped RTESPA-150 probes (0.01–0.025 Ohm-cm). All measurements were acquired over a scan area of 1 μm^2. AFM analysis software (Gwyddion) was used to remove curvature followed by roughness analysis on (n = 3) scans.

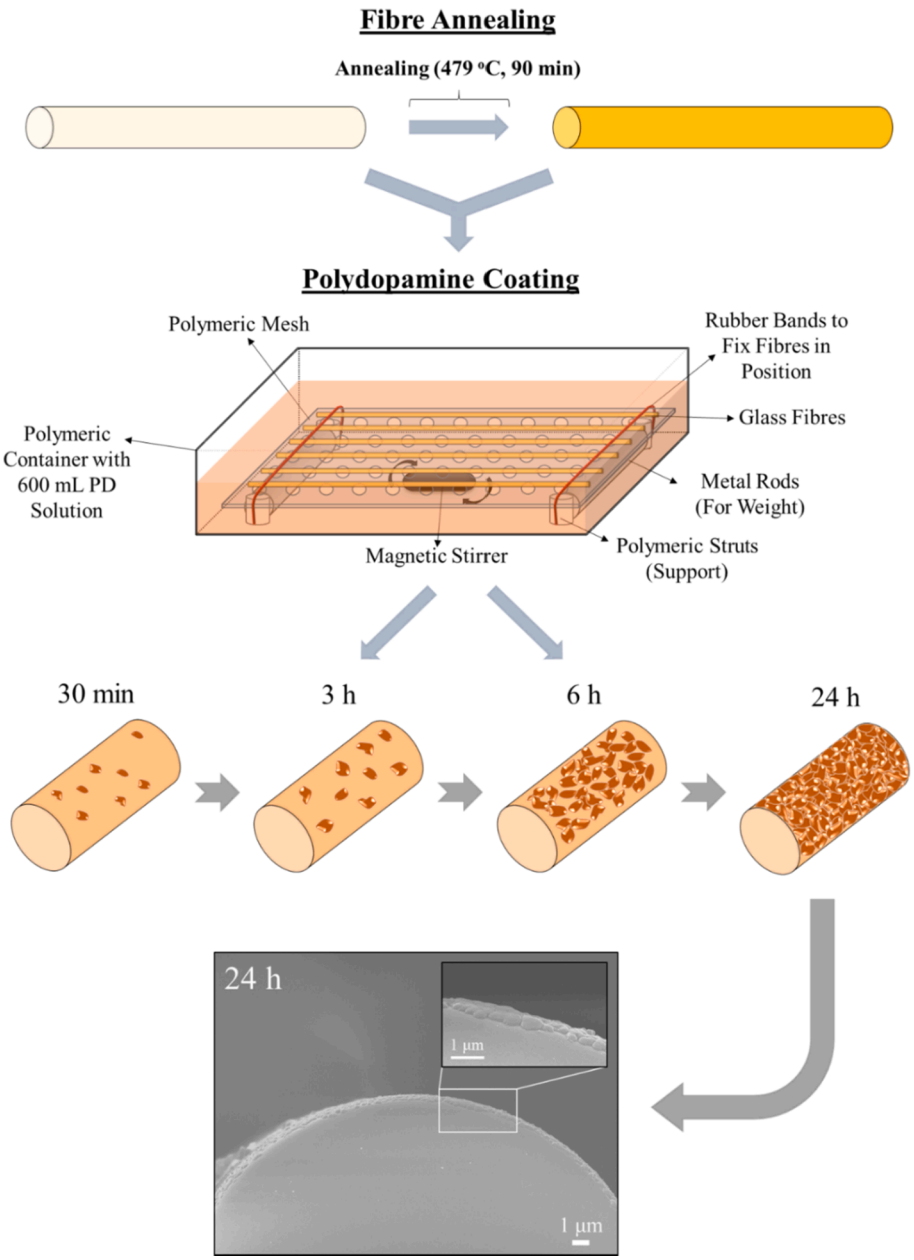

Fig. 1. Schematic of the polydopamine coating process applied to annealed and non-annealed fibres at room temperature. The fibres were secured to a plastic frame to keep them straight. The electron microscope image illustrates the result after 24 h of coating. (For interpretation of the references to colour in this figure legend, the reader is referred to the web version of this article.)

Table 1
Sample codes for composite specimens where NA = non-annealed, NC = non-coated, C = coated, A = annealed.

Code	Fibre type	Fibre coating
NA&NC	35% V_f Non-annealed (NA)	None (NC)
A&NC	35% V_f Annealed (A)	None (NC)
NA&C	35% V_f Non-annealed (NA)	6 h (C)
A&C	35% V_f Annealed (A)	6 h (C)

2.7. Scanning electron microscopy (SEM)

After flexural testing, SEM analysis was conducted on the fibres and cross sections of the composite samples that were sputter-coating with platinum (utilising a SC500, Emscope), to assess the quality of the fibre/matrix interface. Samples were examined using an XL 30 scanning electron microscope (Philips, UK) in secondary electron mode at an accelerating voltage of 10 kV and a working distance of 30 mm.

2.8. Ellipsometry

An estimate of the thickness of the PD coating was obtained by using spectroscopic variable angle ellipsometry VASE (J. A. Woollam M-2000 ellipsometer, USA) over an angle range of 55-65° and a wavelength range of 200–1600 nm. The measurement required a flat surface; hence it was not possible to measure the fibre coatings directly. Instead, microscope glass slides were coated for this purpose. They were coated alongside the PBG fibres for 0.5, 3, 6 and 24 h so that they experienced equivalent coating conditions. The PD coating was modelled as a Cauchy layer [46] and five replicates of each sample (N = 5) were performed.

2.9. Single filament tensile testing (SFTT)

Single filament testing was performed on a Diastron LEX-810 fitted with a 2000 g load cell and combined with a Mitutoyo LSM6200 laser diameter monitor. The tests were made based on BS ISO 11566, using a gauge length of 25 mm and a speed of 0.017 mm/s (~1 mm/min). Calibration of the laser diameter monitor was conducted using a specially prepared set of phosphate fibres with different diameters. The diameter of these fibres was measured via SEM and then used to calibrate the laser system, resulting in an overall error of ±0.3 μm. A sufficient number of specimens were tested to obtain at least 20 results and Grubbs' test was used to check for outliers. Weibull analysis was used at 95% CI to determine a most probable fibre failure strength using Minitab® statistical software.

2.10. Composite degradation study

The composites specimens were subjected to an 8 week degradation study, which was performed in accordance with the standard BS EN ISO 10993-13. Composite samples were placed individually into 30 ml glass vials and 30 ml of Phosphate Buffered Saline (PBS) solution (pH = 7.4 ± 0.2) was added to each vial to fully immerse the sample. The vials were then kept in an oven at 37 °C and the PBS was changed at weekly intervals. Samples were removed for testing at intervals of 1, 3, 7, 14, 28 and 56 days. Change in sample mass was recorded at each time point and the solution pH was measured using a Mettler Toledo pH probe.

2.11. Gel permeation chromatography (GPC)

GPC was performed to analyse the molecular weight and molecular weight distribution of the PCL matrix. The GPC used was an Agilent Technologies 1260 Infinity GPC system with mixed D columns at 40 °C and a refractive index detector. Chloroform was used as the mobile phase at a flow rate of 1.0 cm^3/min and calibration was accomplished against PMMA standards. The calibration range of the GPC was from 10 min to 17.35 min elution time, corresponding to molecular weights from 0.580 to 377.4 kg/mol. Sample concentration was *ca.* 5 mg/ml.

2.12. Composite flexural testing

3-point bending tests were conducted on a Bose ElectroForce® Series II 3330 testing machine. The testing machine is equipped with an environmental chamber, which enables tests within liquid at various temperatures. Flexural tests were performed on both PBS-degraded (up to 8 weeks) and non-degraded samples. All flexural tests were performed in accordance with standard BS EN ISO 14125:1998. Specimen dimensions of 40 mm × 15 mm × 2 mm, a crosshead speed of 1 mm/min and a 3 kN load cell were used. Tests were performed in triplicate (n = 3). Flexural properties of the composites were tested at 37 °C submerged in PBS solution. The samples were immersed for 5 min prior to testing to allow the sample temperature to equilibrate.

3. Results

3.1. Chemical analysis of fibre surface

The presence of the polydopamine coating on the fibres was verified using XPS. The survey spectrum of the control fibre showed photoelectron emissions associated with the phosphate glass composition (see supplementary data Figure S1). High resolution spectra were used to quantify the proportion of the organic components of O, C, N and the inorganic P associated with the glass substrate. The values are provided in Table 2 and Fig. 2 shows the high resolution scans of O 1s, N 1s and P 2p.

Deconvolution of the high resolution O 1s spectrum for the uncoated sample showed two components situated at 533.6 and 531.9 eV. These are associated with P—O—P bridging oxygens (BO) and P—O/P=O non bridging oxygens (NBO) characteristic of phosphate glass structures [47]. The shift in the envelope of O 1s spectra towards higher binding energies was observed from 30 min to 24 h and was assigned to C—O and C=O characteristic of polydopamine formation (Fig. 2 O 1s) [48].

Table 2
XPS analysis of growth of polydopamine layer on the glass fibre surface.

Elements	At%				
	Uncoated	0.5 h	3 h	6 h	24 h
N 1s	0.0	0.8	3.3	3.8	5.1
O 1s	53.3	60.1	46.2	35.0	25.0
C 1s	25.2	17.0	38.5	54.5	66.3
P 2p	21.5	22.1	12.0	6.7	3.6
N/P Ratio	N/A	0.04	0.28	0.57	1.42

Deconvolution of the P 2p positioned at 134.3 eV may be associated with majority PO_3 Q^2 metaphosphate surface species of the phosphate tetrahedral [49]. No significant variation in the positioning of C 1s was observed and was not deconvoluted here, due to the presence of adventitious carbon. High resolution spectra of the N 1s for all coated samples were deconvoluted with a single component positioned from 399.9 to 400.2 eV, which is attributed to the presence of an organic polydopamine matrix (Fig. 2 N 1s) [49].

This compositional analysis showed a proportional increase in the N 1s emissions from (0.0 to 5.1 at%) associated with deposition of the polydopamine, as well as a reduction in P 2p signal from (21.5 to 3.6 at %) attributed to partial shielding of the glass by the newly deposited polydopamine coating. The ratio of N/P has been added to Table 2 as a convenient illustration of these changes. Overall, this is highly suggestive of an increasing thickness of polydopamine with coating time, which obscures the glass fibre surface.

Raman Spectroscopy was used to confirm the formation of polydopamine onto the phosphate glass fibres. Raman spectra for all the samples are presented in Fig. 3.

All samples contained bands associated with the phosphate-based glass fibres from 340 to 1250 cm^{-1}. The band positions [50–52] were allocated to their respective bonds and were shown to remain consistently positioned pre- and post-coating of polydopamine. Similarly, no positional changes were observed following annealing. Scattering at *ca.* 1580 cm^{-1} and 1341 cm^{-1} emerged for the 30 min coatings and intensified with deposition time up to 24 h. The band at 1341 cm^{-1} was associated with stretching of the indole ring or C-N stretching of the polydopamine structure whilst the band at 1580 cm^{-1} was associated with C = C pyrrole ring stretching or deformation of the catechol ring [53,54].

3.2. Surface topography of the fibres

Atomic force micrographs and scanning electron microscopy images were collected for the control and coated fibres (Fig. 4).

The SEM images show the development of particulate features on the fibre surfaces with increasing treatment time. AFM indicates an increasingly rough surface at the 10 s of nanometres scale, with much larger features interspersed. AFM Surface roughness measurements showed increasing roughness (R_a) from 1.4 ± 0.6 nm to 2.6 ± 0.1 nm between the control and 24 h coated samples.

3.3. Ellipsometry

Ellipsometry results for coating microscope glass slides with polydopamine are provided in Fig. 5. For the period up to 6 h the amount of coating increases approximately linearly to reach 18 nm. The rate of deposition then appears to drop off by the 24 h time point with a thickness of 46 nm.

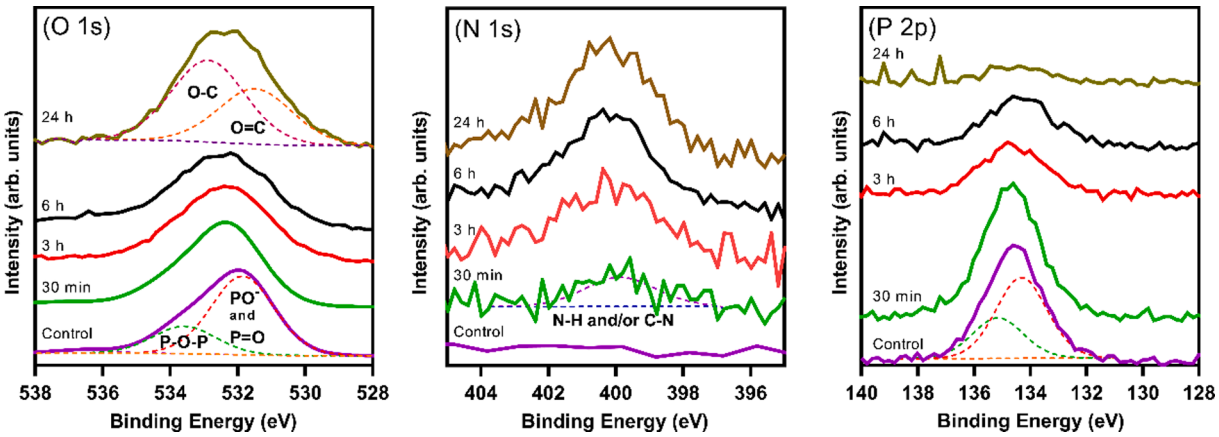

Fig. 2. XPS deconvolution of the uncoated and coated fibres. High resolution of O 1s, N 1s and P 2p show gradual development of polydopamine. (For interpretation of the references to colour in this figure legend, the reader is referred to the web version of this article.)

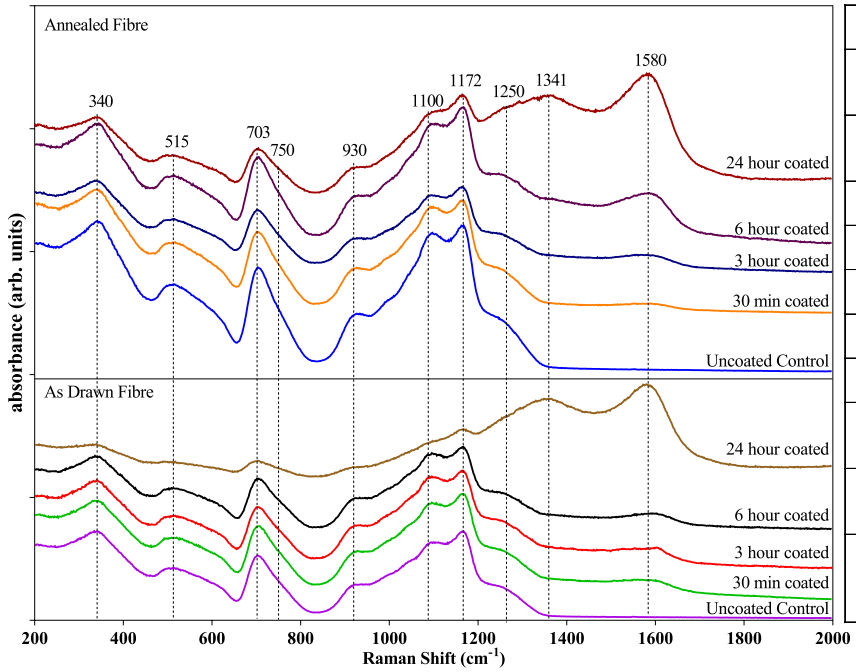

Raman Shift (cm^{-1})	Bonding
340	(O- P- O) bending vibration Non-Bridging Oxygens
515	(P-O) bending vibrations and P-O-P in chain stretching vibrations
703	ν_s(P- O- P) Bridging Oxygens (Q^2)
750	ν_{as}(P- O- P) Bridging Oxygens (Q^2 and Q^1)
930	ν_s(O- P- O) Non-Bridging Oxygens (Q^0)
1100	ν_s(O- P- O) Non-Bridging Oxygens (Q^1)
1172	ν_s(O- P- O) Non-Bridging Oxygens (Q^2)
1250	ν_{as}(O- P- O) Non-Bridging Oxygens (Q^2) and ν_s(P=O)
1341	Stretching of the Polydopamine indole ring or C-N Stretching
1580	Polydopamine C=C pyrrole ring stretching or deformation of the Catechol ring

Fig. 3. Raman scattering spectra of control and polydopamine coated phosphate glass fibres. (For interpretation of the references to colour in this figure legend, the reader is referred to the web version of this article.)

3.4. Single fibre tensile testing (SFTT)

Results for single filament tensile testing are provided in Fig. 6. For the non-annealed fibres there is a significant increase in fibre strength up to 6 h of coating, whereas the annealed fibres show no significant difference in strength at any of the time points. The non-annealed fibres had an average modulus of 50 ± 4 GPa and after annealing, the average modulus of the fibres increased to 61 ± 5 GPa. However, no significant differences in tensile modulus were observed for either annealed or non-annealed fibres after coating for different periods. No particular trend of Weibull modulus (m) was observed, with values from 3.2 to 9.4.

3.5. Composite flexural testing

The results of flexural analysis are provided in Fig. 7. For all samples, the strength drops considerably between dry (day 0) and saturated (day 1) [55]. It can be seen that composites made with fibres that are non-annealed and not coated (NA&NC) lose their properties rapidly, with an almost complete loss in properties after 2 weeks. Application of the polydopamine coating without annealing provides little benefit, with a modicum of improvement (162 MPa and 20 GPa strength and modulus at day 1 for NA&C vs 121 MPa and 14 GPa respectively for NA&NC). This only persists within the first week and almost complete loss occurs again by 2 weeks. Annealing alone provides a noticeable benefit in both strength and modulus out to 56 days but provides retention of only 20% of day 1 properties. By using both annealing and a polydopamine coating, the properties of the composites are maintained at a high level out to at least 56 days. Both strength and modulus are retained at around 70–75% of the day 1 (saturated) properties.

3.6. SEM of the composite cross-sections

SEM of the samples after degradation are shown in Fig. 8.

For both the annealed samples (A&NC and A&C) there is little apparent change in the fibre morphology, though there is an indication of loss of intimate contact between fibre and matrix. For both the non-

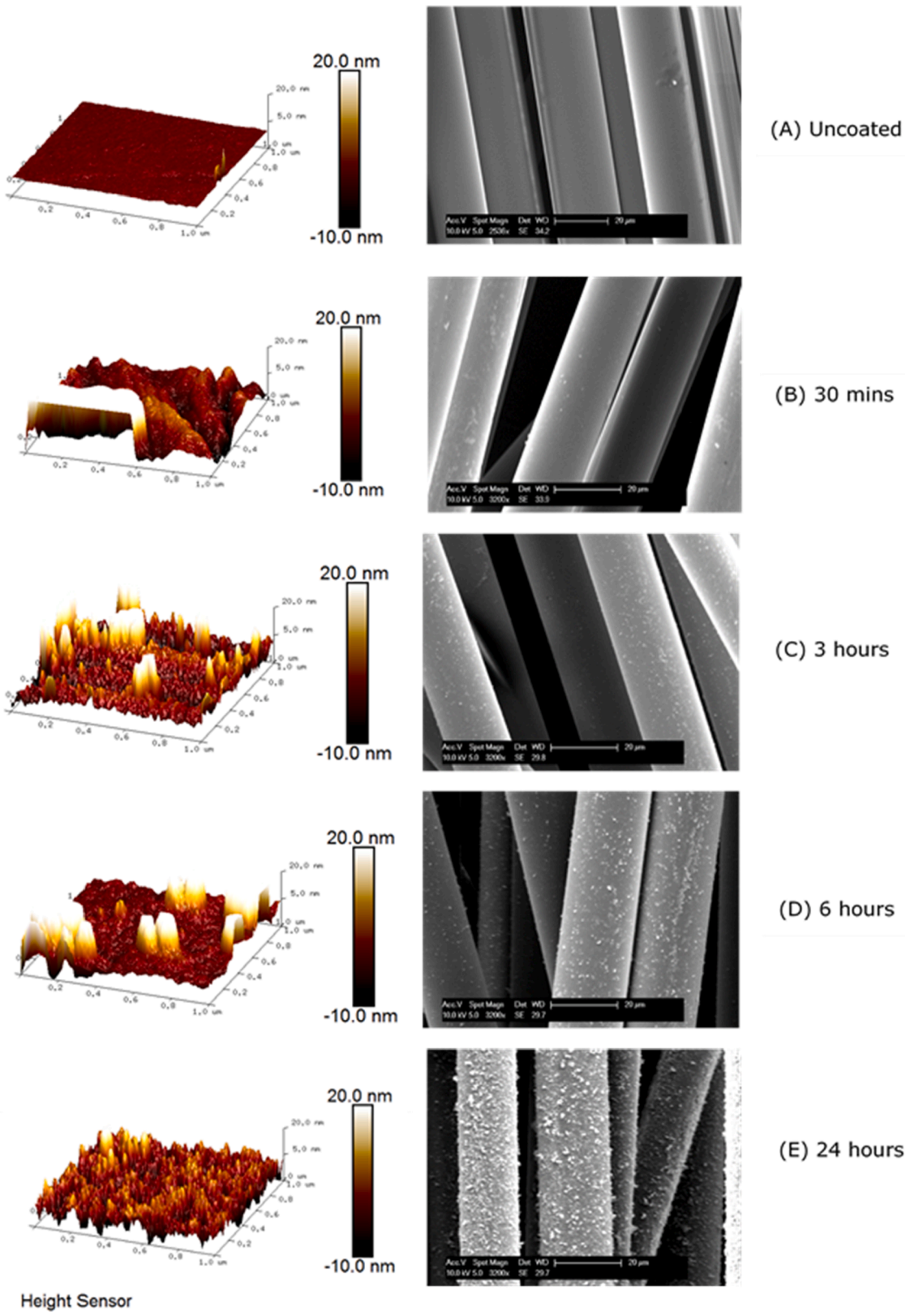

Fig. 4. AFM and SEM micrographs of the coated and uncoated fibres; (A) uncoated, (B) 30 mins coating with polydopamine solution, (C) 3 h, (D) 6 h, (E) 24 h. (For interpretation of the references to colour in this figure legend, the reader is referred to the web version of this article.)

annealed samples (NA&C and NA&NC) there is a distinct change in the fibre morphology, with the occurrence of a micro-tubular structure.

3.7. Degradation properties of the composites

Mass loss, pH values and changes in molecular weight are provided in Fig. 9.

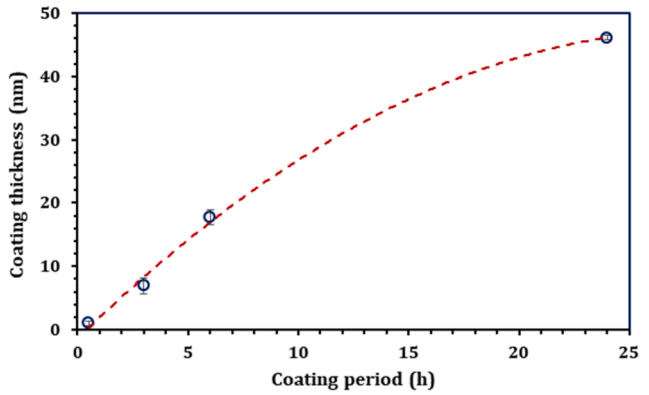

Fig. 5. Ellipsometry of microscope glass slides coated with polydopamine for different periods of time. The dotted line is a guide for the eye and does not imply a relationship. (For interpretation of the references to colour in this figure legend, the reader is referred to the web version of this article.)

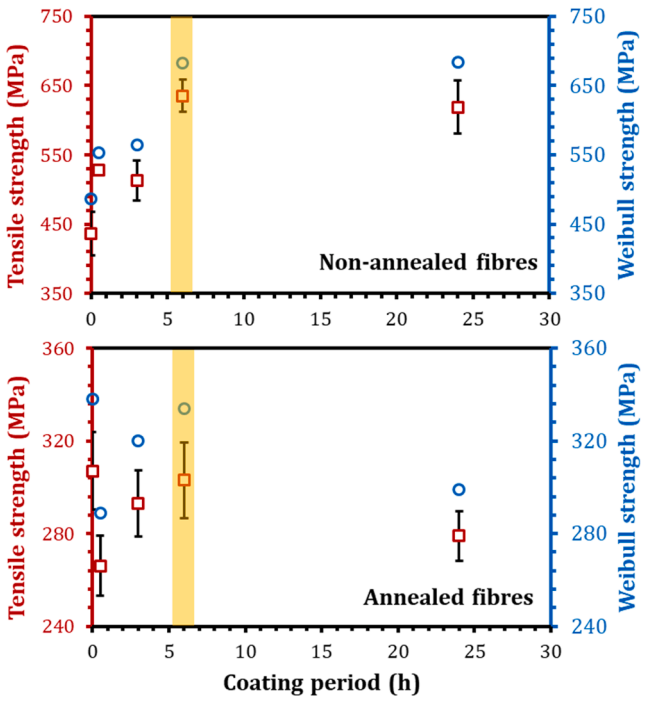

Fig. 6. Tensile properties of non-annealed and annealed fibres after coating with polydopamine for different periods of time. The yellow band shows the coating at 6 h, which was used for the production of composites. (For interpretation of the references to colour in this figure legend, the reader is referred to the web version of this article.)

It can be seen that, while mechanical properties change within the first few days, no significant mass loss is observed until 7–14 days and only then for the non-annealed samples. The pH falls over a similar timescale to the mass loss, which would be expected as breakdown products from the glass are dispersed in the surrounding media. However, the A&NC sample provides little mass loss but does see a significant change in pH. Loss in matrix molecular weight also correlates with mass loss.

4. Discussion

Polydopamine coating has been reported to occur via oxidative polymerization (catechol oxidase to a quinone in the presence of oxygen and followed by polymerization step) of dopamine, similar to melanin

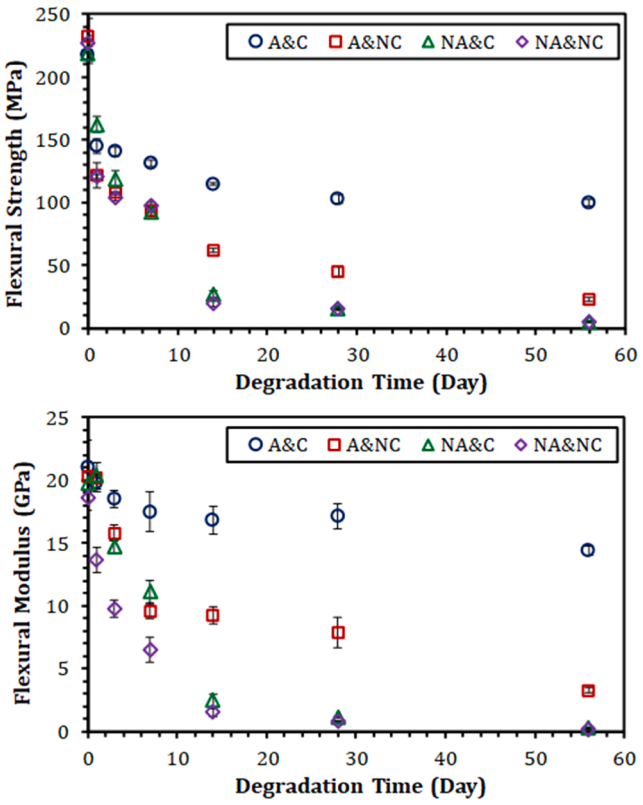

Fig. 7. Flexural strength and modulus for in-situ polymerised phosphate glass/PCL composites subjected to different conditions of annealing and polydopamine coating. Annealed and coated (A&C), annealed and non-coated (A&NC), non-annealed and coated (NA&C), non-annealed and non-coated (NA&NC). (For interpretation of the references to colour in this figure legend, the reader is referred to the web version of this article.)

formation [36]. Lee et al. in 2019 [56] stated that the details of the mechanism of polydopamine coating formation remain an active area of investigation. The presence of polydopamine on the surface of the glass fibres is confirmed by XPS and by Raman spectroscopy (Figs. 2 and 3). Both techniques indicated an increase in the quantity of polydopamine on the fibre surfaces with an increase in coating time. XPS was able to track an increase in nitrogen related to the polydopamine and a decrease in signals related to the glass surface. Raman provided specific identification of bands related to the catechol ring of the polydopamine. The obtained XPS and Raman spectra of polydopamine coating in this study were consistent with the spectra published for polydopamine in powder form [57,58].

The morphology of the coating was investigated through SEM and AFM. The SEM images (Fig. 4) indicate an apparent particulate deposition on the fibre surfaces, with features <2 μm. However, by looking closer at the regions of the fibre between these particulates using AFM it can be seen that there is a coating on the order of 10 s of nm. These together indicate a definitively bimodal coating, though it is not clear if the larger particles form directly on the fibre surface or whether they are precipitate from the solution that has subsequently attached to the fibre. A recent paper by Zhang would suggest the latter [59]. This bimodal coating could potentially provide both an adhesive and a mechanical interlocking mechanism to improve the fibre/matrix interface.

Ellipsometry was used to infer an effective thickness for the polydopamine coating. However, the area of analysis is much larger than a fibre and must be flat. Because of these limitations, the technique could not be applied directly to the fibres. Instead, ellipsometry was performed on glass microscope slides that were placed in the dopamine treatment solution alongside the fibres. The observed thickness was on a par with that seen by Lee et al. [36] (10 s of nm). A correlation was observed

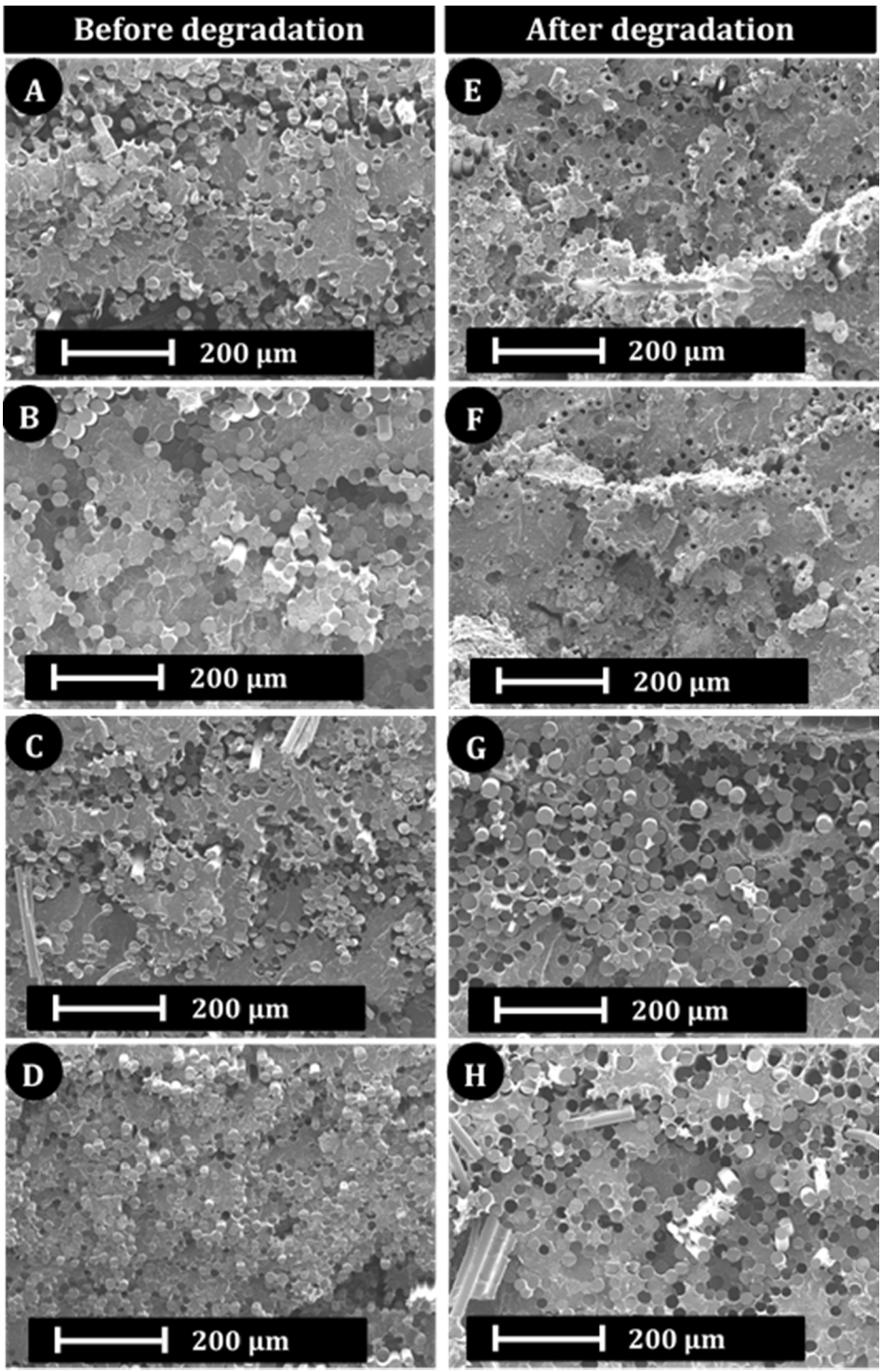

Fig. 8. SEM micrographs of freeze fractured surfaces of PCL-PGF composites containing; (A, E) non-annealed and non-coated fibres, (B, F) non-annealed and coated fibres, (C, G) annealed and non-coated fibres, (D, H) annealed and coated fibres before and after 56 days of degradation in PBS at 37 °C. (For interpretation of the references to colour in this figure legend, the reader is referred to the web version of this article.)

between XPS data (percentage of surface N) and the ellipsometry thickness measurement (Fig. 10).

This correlation is in good agreement with the depth penetration observed for XPS (*ca.* 5–10 nm [60]. As the deposition time increases for the polydopamine treatment, a thicker layer is detected by both the ellipsometry (Fig. 5) and XPS (Table 2) techniques. At the early stages up to 3 h the XPS was not able to effectively resolve the nitrogen peaks (Fig. 2) and so the correlation in Fig. 10 does not hold below 5 nm. This may be due to lack of sufficient coating, or a non-homogeneous coating. Based on the ellipsometry, coating times of more than 3 h produce polydopamine thicknesses in excess of 5 nm, which is quantifiable via XPS.

The XPS data also indicates that phosphorus is still present at 24 h, when the coating is in theory >40 nm. This could indicate a porous or incomplete coating, such that some glass fibre surface is still observable. It is likely that there is a degree of porosity to the coating, since over time

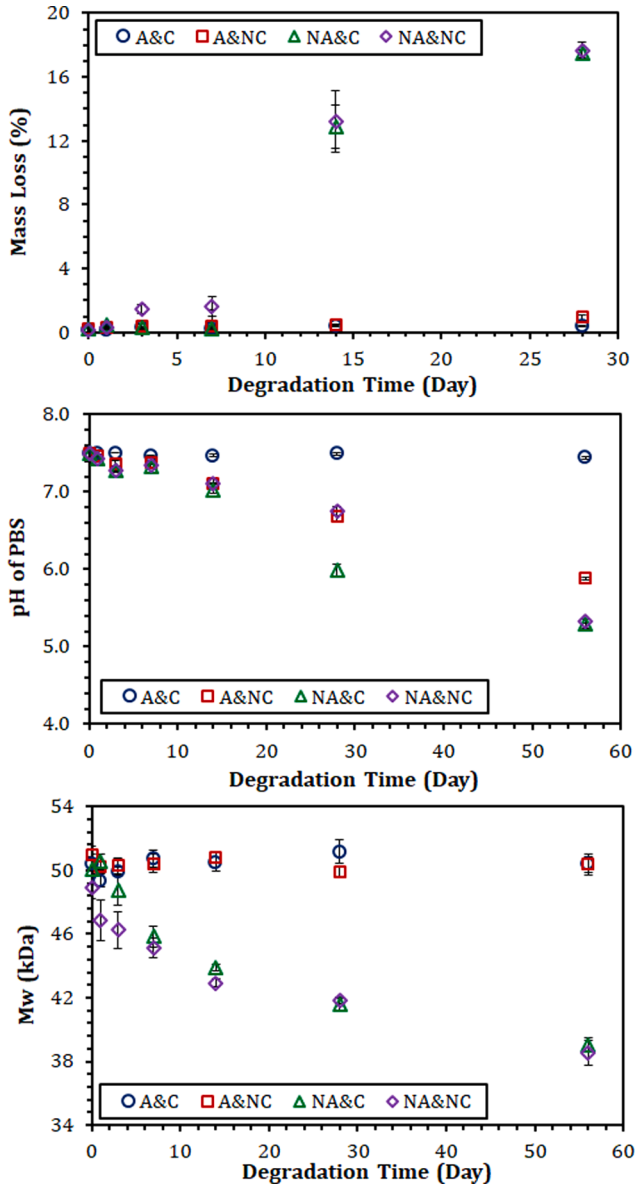

Fig. 9. Mass loss, pH values and changes in molecular weight for in-situ polymerised phosphate glass/PCL composites subjected to different conditions of annealing and polydopamine coating. Annealed and coated (A&C), annealed and non-coated (A&NC), non-annealed and coated (NA&C), non-annealed and non-coated (NA&NC). (For interpretation of the references to colour in this figure legend, the reader is referred to the web version of this article.)

water can ingress and cause fibre degradation (particularly for the non-annealed and coated fibre (NA&C)). However, it seems unlikely that a photoelectron could find a direct pathway through. A crack caused by shrinkage or other means is more likely.

Alternatively, since the polydopamine coating process is aqueous and the fibres water soluble, a degradation of the fibre could be anticipated during the coating, before the protective surface develops. Some of the degradation product may become incorporated into the coating structure, which could explain the P still present in the XPS results of the thicker coatings.

The magnitude of this potential degradation during coating was assessed using single filament tensile testing. The results for the analysis for both annealed and non-annealed fibres are provided in Fig. 6. Values of strength and modulus for the uncoated fibres were consistent with observations from previous studies [61–64]. Although the amount of polydopamine applied to the surface of the fibre appears to increase with

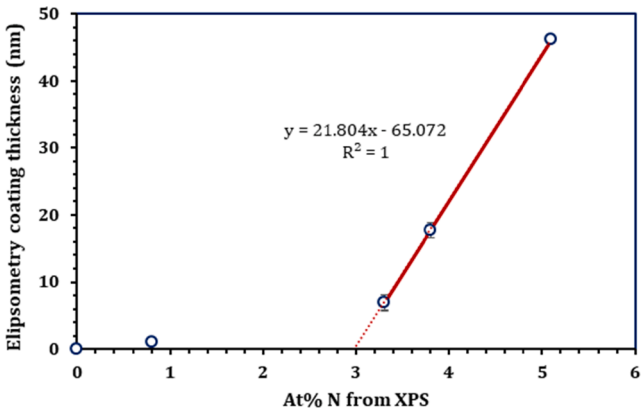

Fig. 10. Correlation between thickness (determined by ellipsometry) and surface nitrogen percentage (from XPS), indicating a linear correlation above 3% nitrogen. (For interpretation of the references to colour in this figure legend, the reader is referred to the web version of this article.)

coating time for both annealed and non-annealed fibres, the effect on fibre properties was less straightforward. Instead of seeing a drop in fibre properties with immersion time there was an increase in strength for certain samples. For the annealed fibres there was no statistical difference in strength values ($P = 0.05$). However, for the non-annealed fibres there was a surprising and significant ($P = 0.05$) increase in strength up to 6 h of coating, though there was no further increase up to 24 h.

Glass fibre strength is a flaw dominated event [65] and so the improvement in strength for the coated, non-annealed samples could indicate that the coating is sufficient to bridge, or otherwise protect, those flaws to some extent by increasing the effective crack tip radii and reducing stress concentrations [66]. Although it can benefit long term degradation behaviour, it is known that annealing (heat treatment) causes a significant drop in glass fibre strength [35], suggesting an exacerbation of surface flaws beyond those of the non-annealed fibre. This can be seen in the comparison of day 0 fibre properties in Fig. 6, where the annealed fibre strength is much lower than the non-annealed (338 vs 487 MPa). No significant increase in strength after coating would suggest that while the polydopamine can bridge flaws in the non-annealed fibre, the flaws in the annealed are too extensive to be fully bridged, at least at the level of coating obtained in this study. In a parallel study by the authors, annealed fibres of phosphate glass were subjected to a strength recovery treatment before coating [67]. That study indicated that significant strength recovery could be achieved prior to the polydopamine coating by using an acid etch. The three-stage treatment that it considered (annealing, etching, coating) could be incorporated into future composite studies to achieve higher overall composite mechanical properties.

To test the effectiveness of polydopamine as a coupling agent in absorbable systems, composite parts were produced and tested. Although there was a continual increase in coating thickness with time, a 6 h coating treatment was selected. This balanced an increase in fibre strength with a limitation on fibre exposure to aqueous solution. While this may not be the exact optimum solution, it was sufficient to demonstrate the effectiveness of the coating. PLA/phosphate glass composites of 35% fibre volume fraction were produced by in-situ polymerisation. In-situ polymerisation has been shown to have a significantly better interfacial bonding than laminate stacking by virtue of improved fibre wetting [17].

The mechanical data in Fig. 7 indicate that all samples experienced an initial drop in strength over the first day. While potentially this could be related to a degree of interfacial breakdown, it is also at least partially attributed to a plasticisation of the polymer matrix by water [68] and the temperature of testing [69,70]. The annealed and non-coated (AN&NC)

fibres provided a better retention of composite properties than either of the non-annealed samples. At later time points, the annealed and coated (A&C) fibres provided much improved retention of both strength and modulus (70–75% of day 1 properties by 56 days) in comparison to the other samples; A&NC less than 20% and both NA samples were less than 10% of the initial day 1 properties by 56 days.

This is supported by SEM observations (Fig. 8). For the non-annealed fibres there is gross distortion of the fibre shape and an apparently empty core. This phenomenon has been observed previously [16,17,28,31,71] and, while not conclusively established, is thought to be a dissolution/re-precipitation of breakdown products due to high localised solution concentration. The central empty core may be as a result of pull out of the remaining, undissolved core.

Mass loss and pH studies (Fig. 9) also indicate a considerable breakdown of the non-annealed fibres, with the loss of 18% mass and a drop to pH 5 by 56 days. Further, the polymer molecular weight loss was highly significant, with the non-annealed samples showing a loss of approximately 25% by 56 days. No significant molecular weight loss was observed for the annealed samples, suggesting that the breakdown products of the fibres were primarily responsible for this molecular weight loss due to acid catalysis [72].

In summary, while annealing or polydopamine coating in isolation provided little benefit to property retention, the combination of both provided a very significant improvement. This manifested particularly in the retention of composite wet strength out to 8 weeks, which meets the target for bone healing for at least the upper extremities. This target has not been achieved by any previous phosphate glass fibre coupling agent treatment of which the authors are aware. This is an extremely encouraging result and future studies will look at the effectiveness of the treatment in other polymer matrix types and when using more commercially applicable manufacturing techniques such as compression moulding.

5. Conclusions

Polydopamine can be applied to the surface of a phosphate-based glass fibre by using a simple coating method. The presence of the coating can be verified through its nitrogen content using XPS and Raman surface techniques. Based on ellipsometry, AFM and SEM data the coating appears to be bimodal, with a very thin (10 s of nanometres) coating combined with scattered particulates on the order of microns in size. While the coating appears to provide some improvement in dry fibre properties for non-annealed fibres, this does not translate to observations in the composites. The coating alone does not provide an improvement in composite property retention, but the combination of annealing and coating provides a synergistic improvement. This is the first example of long-term retention of wet strength properties observed for phosphate-based glass fibre composites, falling within the target range for bone healing (6–12 weeks).

CRediT authorship contribution statement

Reda M. Felfel: Conceptualization, Funding acquisition, Project administration, Resources, Supervision, Methodology, Investigation, Data curation, Formal analysis, Writing - original draft, Writing - review & editing. **Andrew J. Parsons:** Conceptualization, Funding acquisition, Project administration, Resources, Supervision, Methodology, Investigation, Data curation, Formal analysis, Writing - original draft, Writing - review & editing. **Menghao Chen:** Methodology, Investigation, Data curation, Writing - review & editing. **Bryan W. Stuart:** Methodology, Investigation, Data curation, Writing - review & editing. **Matthew D. Wadge:** Methodology, Investigation, Data curation, Writing - review & editing. **David M. Grant:** Conceptualization, Funding acquisition, Project administration, Resources, Supervision, Writing - review & editing.

Declaration of Competing Interest

The authors declare that they have no known competing financial interests or personal relationships that could have appeared to influence the work reported in this paper.

Acknowledgements

This work was supported by the Engineering and Physical Sciences Research Council (grant number EP/L022494/1), Nottingham Hermes Fellowship (16a/I) funded by the Higher Education Innovation Fund (HEIF) and the Nottingham Impact Accelerator (EP/R511730/1). The authors acknowledge the use of facilities at the Nanoscale and Microscale Research Centre.

Appendix A. Supplementary material

Supplementary data to this article can be found online at https://doi.org/10.1016/j.compositesa.2021.106415.

References

[1] Abou Neel EA, Salih V, Knowles JC. Phosphate-Based Glasses. In: Ducheyne P, editor. Comprehensive biomaterials. Elsevier; 2011. p. 285–97.
[2] Brauer DS. Phosphate Glasses. In: Jones JR, Clare AG, editors. Bio-Glasses: An Introduction. John Wiley & Sons, Ltd.; 2012. p. 45–64.
[3] Brauer DS, Rüssel C, Vogt S, Weisser J, Schnabelrauch M. Degradable phosphate glass fiber reinforced polymer matrices: Mechanical properties and cell response. J Mater Sci - Mater Med 2008;19(1):121–7.
[4] Chakladar ND, Harper LT, Parsons AJ. Optimisation of composite bone plates for ulnar transverse fractures. J Mech Behav Biomed Mater 2016;57:334–46.
[5] Chen M, Lu J, Felfel RM, Parsons AJ, Irvine DJ, Rudd CD, et al. Wet and dry flexural high cycle fatigue behaviour of fully bioresorbable glass fibre composites: In-situ polymerisation versus laminate stacking. Compos Sci Technol 2017;150:1–15.
[6] Colquhoun R, Tanner KE. Mechanical behaviour of degradable phosphate glass fibres and composites-a review. Biomed Mater 2016;11(1).
[7] Kobayashi HYLS, Brauer DS, Rüssel C. Mechanical properties of a degradable phosphate glass fibre reinforced polymer composite for internal fracture fixation. Mater Sci Eng: C 2010;30(7):1003–7.
[8] Hossain KMZ, Felfel RM, Grant DM, Ahmed I. Phosphate Glass Fibres and Their Composites. In: Boccaccini AR, Brauer DS, Hupa L, editors, Bioactive Glasses: Fundamentals, Technology and Applications, Royal Society of Chemistry; 2017. p. 257–285.
[9] Knowles JC. Phosphate based glasses for biomedical applications. J Mater Chem 2003;13(10):2395–401.
[10] Zhu C, Ahmed I, Parsons AJ, Wang Y, Tan C, Liu J, et al. Novel bioresorbable phosphate glass fiber textile composites for medical applications. Polym Compos 2017.
[11] Bunker BC, Arnold GW, Wilder JA. Phosphate glass dissolution in aqueous solutions. J Non-Cryst Solids 1984;64(3):291–316.
[12] Bunker BC, Casey WH. The Aqueous Chemistry of Oxides. Oxford University Press; 2016.
[13] Ma L, Brow RK, Schlesinger ME. Dissolution behavior of Na2O-FeO-Fe2O3-P2O5 glasses. J Non-Cryst Solids 2017;463(1):90–101.
[14] Felfel RM, Ahmed I, Parsons AJ, Palmer G, Sottile V, Rudd CD. Cytocompatibility, degradation, mechanical property retention and ion release profiles for phosphate glass fibre reinforced composite rods. Mater Sci Eng, C: Mater Biol Appl 2013;33(4):1914–24.
[15] Kobayashi HYLS, Brauer DS, Rüssel C. Mechanical properties of a degradable phosphate glass fibre reinforced polymer composite for internal fracture fixation. Mater Sci Eng, C 2010;30(7):1003–7.
[16] Sharmin N, Hasan MS, Parsons AJ, Rudd CD, Ahmed I. Cytocompatibility, mechanical and dissolution properties of high strength boron and iron oxide phosphate glass fibre reinforced bioresorbable composites. J Mech Behav Biomed Mater 2016;59:41–56.
[17] Chen M, Parsons AJ, Felfel RM, Rudd CD, Irvine DJ, Ahmed I. In-situ polymerisation of fully bioresorbable polycaprolactone/phosphate glass fibre composites: In vitro degradation and mechanical properties. J Mech Behav Biomed Mater 2016;59:78–89.
[18] Ruedi T, Buckley R, Moran C. AO Principles of Fracture Management, Books and DVD, AO; 2007.
[19] Ageyeva T, Sibikin I, Karger-Kocsis J. Polymers and Related Composites via Anionic Ring-Opening Polymerization of Lactams: Recent Developments and Future Trends. Polymers 2018;10(4):357.
[20] Nguyen NT, Greenhalgh E, Kamaruddin MJ, El Harfi J, Carmichael K, Dimitrakis G, et al. Understanding the acceleration in the ring-opening of lactones delivered by microwave heating. Tetrahedron 2014;70(4):996–1003.
[21] Plueddemann EP. Silane Coupling Agents. US, New York: Springer; 1991.

[22] Thomason JL. Glass Fibre Sizing. J.L., Glasgow: Thomason; 2015.
[23] Andriano KP, Daniels AU, Heller J. Effectiveness of silane treatment on absorbable microfibers. J Appl Biomater 1992;3(3):191–5.
[24] Cozien-Cazuc S. Characterisation of resorbable phosphate glass fibres, Engineering. Nottingham: University of Nottingham; 2006.
[25] Haque P, Parsons AJ, Barker IA, Ahmed I, Irvine DJ, Walker GS, et al. Interfacial properties of phosphate glass fibres/PLA composites: Effect of the end functionalities of oligomeric PLA coupling agents. Compos Sci Technol 2010;70 (13):1854–60.
[26] Hasan MS, Ahmed I, Parsons AJ, Walker GS, Scotchford CA. The influence of coupling agents on mechanical property retention and long-term cytocompatibility of phosphate glass fibre reinforced PLA composites. J Mech Behav Biomed Mater 2013;28:1–14.
[27] Khan RA, Parsons AJ, Jones IA, Walker GS, Rudd CD. Effectiveness of 3-Amino-propyl-Triethoxy-Silane as a Coupling Agent for Phosphate Glass Fiber-Reinforced Poly(caprolactone)-based Composites for Fracture Fixation Devices. J Thermoplast Compos Mater 2011;24(4):517–34.
[28] Yang J. Preparation and characterisation of a bioresorbable phosphate glass fibre reinforced poly(ε-caprolactone) composite, Engineering. Nottingham: University of Nottingham; 2007. p. 182.
[29] Haque P, Barker IA, Parsons AJ, Thurecht KJ, Ahmed I, Walker GS, et al. Influence of Compatibilizing Agent Molecular Structure on the Mechanical Properties of Phosphate Glass Fiber-Reinforced PLA Composites. J Polym Sci, Part A: Polym Chem 2010;48(14):3082–94.
[30] Khan RA, Parsons AJ, Jones IA, Walker GS, Rudd CD. Surface treatment of phosphate glass fibers using 2-hydroxyethyl methacrylate: Fabrication of polycaprolactone based composites. J Appl Polym Sci 2009;111(1):246–54.
[31] Liu X, Grant DM, Palmer G, Parsons AJ, Rudd CD, Ahmed I. Magnesium coated phosphate glass fibers for unidirectional reinforcement of polycaprolactone composites. J Biomed Mater Res B Appl Biomater 2015;103B:1424–32.
[32] Perera MS. The use of sorbitol-initiated polylactic acid as a coupling agent in resorbable phosphate glass fibre reinforced polylactic acid composites, Engineering. Nottingham: University of Nottingham; 2015. p. 195.
[33] Cozien-Cazuc S, Parsons AJ, Walker GS, Jones IA, Rudd CD. Real-time Dissolution of P40Na20Ca16Mg24 Phosphate Glass Fibres. J Non-Cryst Solids 2009;355 (50–51):2514–21.
[34] Ibnabddjalil M, Loh I-H, Chu CC, Blumenthal N, Alexander H, Turner D. Effect of surface plasma treatment on the chemical, physical, morphological, and mechanical properties of totally absorbable bone internal fixation devices. J Biomed Mater Res Part A 1994;28(3):289–301.
[35] Thomason JL, Jenkins P, Yang L. Glass Fibre Strength—A Review with Relation to Composite Recycling. Fibers 2016;4(2):18.
[36] Lee H, Dellatore SM, Miller WM, Messersmith PB. Mussel-Inspired Surface Chemistry for Multifunctional Coatings. Science 2007;318(5849):426–30.
[37] Chen S, Cao Y, Feng J. Polydopamine As an Efficient and Robust Platform to Functionalize Carbon Fiber for High-Performance Polymer Composites. ACS Appl Mater Interfaces 2014;6(1):349–56.
[38] Fu S, Yu B, Duan L, Bai H, Chen F, Wang K, et al. Combined effect of interfacial strength and fiber orientation on mechanical performance of short Kevlar fiber reinforced olefin block copolymer. Compos Sci Technol 2015;108:23–31.
[39] Li Y, Chen Q, Yi M, Zhou X, Wang X, Cai Q, et al. Effect of surface modification of fiber post using dopamine polymerization on interfacial adhesion with core resin. Appl Surf Sci 2013;274:248–54.
[40] Liu Y, Fang Y, Qian J, Liu Z, Yang B, Wang X. Bio-inspired polydopamine functionalization of carbon fiber for improving the interfacial adhesion of polypropylene composites. RSC Adv 2015;5:107652–61.
[41] Yi M, Sun H, Zhang H, Deng X, Cai Q, Yang X. Flexible fiber-reinforced composites with improved interfacial adhesion by mussel-inspired polydopamine and poly (methyl methacrylate) coating. Mater Sci Eng, C 2016;58:742–9.
[42] Zhou M, Xu S, Li Y, He C, Jin T, Wang K, et al. Transcrystalline formation and properties of polypropylene on the surface of ramie fiber as induced by shear or dopamine modification. Polymer 2014;55(13):3045–53.
[43] Christian P, Jones IA, Rudd CD, Campbell RI, Corden TJ. Monomer transfer moulding and rapid prototyping methods for fibre reinforced thermoplastics for medical applications. Compos A Appl Sci Manuf 2001;32(7):969–76.
[44] Corden TJ, Jones IA, Rudd CD, Christian P, Downes S. Initial development into a novel technique for manufacturing a long fibre thermoplastic bioabsorbable composite: in-situ polymerisation of poly-ϵ-caprolactone. Compos A Appl Sci Manuf 1999;30(6):737–46.
[45] Jiang G, Evans ME, Jones IA, Rudd CD, Scotchford CA, Walker GS. Preparation of poly(ε-caprolactone)/continuous bioglass fibre composite using monomer transfer moulding for bone implant. Biomaterials 2005;26(15):2281–8.
[46] Nirasay S, Badia A, Leclair G, Claverie JP, Marcotte I. Polydopamine-Supported Lipid Bilayers. Materials 2012;5(12):2621–36.
[47] Brow RK. An XPS study of oxygen bonding in zinc phosphate and zinc borophosphate glasses. J Non-Cryst Solids 1996;194(3):267–73.
[48] Zangmeister RA, Morris TA, Tarlov MJ. Characterization of Polydopamine Thin Films Deposited at Short Times by Autoxidation of Dopamine. Langmuir 2013;29: 8619–28.
[49] Wagner CD, Muilenberg GE. Handbook of x-ray photoelectron spectroscopy: a reference book of standard data for use in x-ray photoelectron spectroscopy, Physical Electronics Division. Eden Prairie, Minn: Perkin-Elmer Corp; 1979.
[50] Le Saout G, Simon P, Fayon F, Blin A, Vaills Y. Raman and infrared study of $(PbO)_x(P2O5)_{(1-x)}$ glasses. J Raman Spectrosc 2002;33:740–6.
[51] Moguš-Milanković A, Gajović A, Šantić A, Day DE. Structure of sodium phosphate glasses containing Al_2O_3 and/or Fe_2O_3. Part I. J Non-Cryst Solids 2001;289(1–3): 204–13.
[52] Yadav AK, Singh P. A review of the structures of oxide glasses by Raman spectroscopy. RSC Adv 2015;5:67583–609.
[53] Feng J, Fan H, Zha D, Wang L, Jin Z. Characterizations of the Formation of Polydopamine-Coated Halloysite Nanotubes in Various pH Environments. Langmuir 2016;32:10377–86.
[54] Lin Y-C, Hsub Y-N, Chung Y-C. Bio-inspired HDPE-based dry adhesives and their layer-by-layer catechol modification on the surface for use in humid environments. RSC Adv 2014;4:22931–7.
[55] Felfel RM, Ahmed I, Parsons AJ, Walker GS, Rudd CD. In vitro degradation, flexural, compressive and shear properties of fully bioresorbable composite rods. J Mech Behav Biomed Mater 2011;4(7):1462–72.
[56] Lee HA, Ma Y, Zhou F, Hong S, Lee H. Material-Independent Surface Chemistry beyond Polydopamine Coating. Acc Chem Res 2019;52(3):704–13.
[57] Zou Y, Chen X, Yang P, Liang G, Yang Y, Gu Z, et al. Regulating the absorption spectrum of polydopamine. Sci Adv 2020;6(36):eabb4696.
[58] Mallinson D, Mullen AB, Lamprou DA. Probing polydopamine adhesion to protein and polymer films: microscopic and spectroscopic evaluation. J Mater Sci 2018;53 (5):3198–209.
[59] Zhang C, Lv Y, Qiu W-Z, He A, Xu Z-K. Polydopamine Coatings with Nanopores for Versatile Molecular Separation. ACS Appl Mater Interfaces 2017;9(16):14437–44.
[60] Hantsche H. Comparison of basic principles of the surface-specific analytical methods: AES/SAM, ESCA (XPS), SIMS, and ISS with X-ray microanalysis, and some applications in research and industry. Scanning 1989;11(6):257–80.
[61] Muñoz-Senovilla L, Muñoz F, Tricot G, Ahmed I, Parsons AJ. Structure–properties relationships in fibre drawing of bioactive phosphate glasses. J Mater Sci 2017;52 (15):9166–78.
[62] Sharmin N, Parsons AJ, Rudd CD, Ahmed I. Effect of boron oxide addition on fibre drawing, mechanical properties and dissolution behaviour of phosphate-based glass fibres with fixed 40, 45 and 50 mol% P2O5. J Biomater Appl 2014;29(5): 639–53.
[63] Liu X, Grant DM, Parsons AJ, Harper LT, Rudd CD, Ahmed I. Magnesium Coated Bioresorbable Phosphate Glass Fibres: Investigation of the Interface between Fibre and Polyester Matrices. Biomed Res Int 2013;2013:735981.
[64] Sharmin N, Rudd CD, Parsons AJ, Ahmed I. Structure, viscosity and fibre drawing properties of phosphate-based glasses: effect of boron and iron oxide addition. J Mater Sci 2016;51(16):7523–35.
[65] Griffith AA. The Phenomena of Rupture and Flow in Solids. Philos Trans Roy Soc 1921;221:163–98.
[66] Zinck P, Pay M, Rezakhanlou R, Gerard J-F. Mechanical characterisation of glass fibres as an indirect analysis of the effect of surface treatment. J Mater Sci 1999;34: 2121–33.
[67] Parsons AJ, Felfel RM, Wadge MD, Grant DM. Improved phosphate-based glass fiber performance achieved through acid etch/polydopamine treatment. Int J Appl Glass Sci 2020;11(1):35–45.
[68] Aitchison GA, Walker GS, Jones IA, Rudd CD. Modeling changes in the modulus of poly(ε-caprolactone) due to hydrolysis and plasticization. J Appl Polym Sci 2008; 107(6):3484–90.
[69] Khan RA, Parsons AJ, Jones IA, Walker GS, Rudd CD. Degradation and Interfacial Properties of Iron Phosphate Glass Fiber-Reinforced PCL-Based Composite for Synthetic Bone Replacement Materials. Polym-Plast Technol Eng 2010;49(12): 1265–74.
[70] Mohammadi MS, Ahmed I, Muja N, Almeida S, Rudd CD, Bureau MN, et al. Effect of Si and Fe doping on calcium phosphate glass fibre reinforced polycaprolactone bone analogous composites. Acta Biomater 2012;8(4):1616–26.
[71] Han N, Ahmed I, Parsons AJ, Harper L, Scotchford CA, Scammell BE, et al. Influence of screw holes and gamma sterilization on properties of phosphate glass fiber-reinforced composite bone plates. J Biomater Appl 2013;27(8):990–1002.
[72] Woodruff MA, Hutmacher DW. The return of a forgotten polymer—Polycaprolactone in the 21st century. Prog Polym Sci 2010;35(10): 1217–56.